COMMUNICATIONS IN NUMERICAL METHODS IN ENGINEERING

Commun. Numer. Meth. Engng 2000; **00**:1–6 *Prepared using* cnmauth.cls *[Version: 2002/09/18 v1.02]*

Significance of Equal Principal Stretches in Computational Hyperelasticity

Boris Jeremić and Zhao Cheng

Department of Civil and Environmental Engineering, University of California, Davis, CA, 95616, U.S.A.

Vol. 21, Issue 9, pp 477-486, September 2005

SUMMARY

The computational significance of the case of two or three equal principal stretches in large deformation analysis is investigated in this paper. A detailed analytical study shows that the previously suggested solutions, based on numerical perturbations, are not adequate and might lead to erroneous results. A number of examples are presented to illustrate the approach.

*Correspondence to: Boris Jeremić, Department of Civil and Environmental Engineering, One Shields Ave., University of California, Davis, CA, 95616, U.S.A. jeremic@ucdavis.edu

Contract/grant sponsor: NSF–PEER ; NSF; contract/grant number: EEC-9701568; CMS-0337811

Copyright © 2000 John Wiley & Sons, Ltd.

1. INTRODUCTION

An objective computational treatment of large deformation inelastic problems has been developed recently by using multiplicative decomposition of the deformation gradient (eg. Lee and Liu [6]). The techniques are based on the hyperelastic–plastic approach and most of them stem from pioneering work by Simo et al. [16, 13, 14, 15]. A consistent hyperelastic computational formulation forms a basis of all the developments for large deformation hyperelasto–plasticity. Of particular importance is that the computational formulation can be verified on a complete stress and strain space. This requirement fits well with a much wider goal of computational validation of the developed simulations tools (eg. Oberkampf et al. [9] and Roach [12]).

In this paper a peculiar (yet frequently present) case when two or all three principal stretches are equal is explored. Of particular interest is the computational treatment of the consistent tangent stiffness tensor and stress measures (second Piola–Kirchhoff for example) for this case. The paper is organized around consistent and detailed derivations of large deformation measures, large deformation stress measures and the resulting consistent tangent stiffness tensor. The special cases of equal stretches are dealt with within the derivations, following the general case of all non–equal stretches. The derivations are general as they apply to any hyperelastic material model, including those that are deviatoric only (isochoric), volumetric only and those that can produce both types of responses.

It should be noted that Simo and Taylor [18] did address the issue of two or three equal principal stretches but it was specifically done for the Ogden (deviatoric only) hyperelastic material model and in an Eulerian form. It will also be shown that the method of perturbations suggested later (eg. Simo [15]) can only be applied in a limited number of cases. As it turns out, a solution for the treatment of equal principal stretches based on perturbations can lead to erroneous results and is dependent on the numerical precision of computations. Results for cases of two or three equal principal stretches, obtained using the present approach, are shown. In order to provide a self–sufficient treatment of hyperelasticity, derivatives used to obtain stress measures and consistent tangent stiffness tensors for a number of hyperelastic models are given in the appendix.

2. HYPERELASTICITY

This section develops analytical forms for the deformation tensor, stress measures and the stiffness tensor for general case (non–equal principal stretches) and for two special cases with two and/or three equal principal stretches.

2.1. Deformation Tensor

The deformation tensor† in material (Lagrangian) description, given as C^m_{IJ} $(m = 0, \pm 1, \pm 2, \cdots)$ can be expressed in terms of its eigenvalues and eigenvectors (eg. Ting [19] and Morman [8]) which in case of three different principal stretches ($\lambda_1 \neq \lambda_2 \neq \lambda_3$) can be written as:

$$C^m_{IJ} = \lambda_1^{2m} N_I^{(1)} N_J^{(1)} + \lambda_2^{2m} N_I^{(2)} N_J^{(2)} + \lambda_3^{2m} N_I^{(3)} N_J^{(3)} \tag{1}$$

†Indicial notation is used throughout this paper. Einstein tensor summation is assumed and applies to all pairs of dummy indices. The upper case indices describe the undeformed while lower case indices describe deformed configuration. It is also noted that no summation is implied over indices in parenthesis.

Prepared using cnmauth.cls

The explicit form for the cross product of deformation tensor's unit eigenvectors $N_I^{(A)} N_J^{(A)}$ can then be expressed as:

$$N_I^{(A)} N_J^{(A)} = \lambda_{(A)}^2 M_{IJ}^{(A)} \tag{2}$$

with

$$D_{(A)} = (\lambda_{(A)}^2 - \lambda_{(B)}^2)(\lambda_{(A)}^2 - \lambda_{(C)}^2) = 2\lambda_{(A)}^4 - I_1 \lambda_{(A)}^2 + I_3 \lambda_{(A)}^{-2} \tag{3}$$

$$M_{IJ}^{(A)} = \frac{C_{IJ} - \left(I_1 - \lambda_{(A)}^2\right) \delta_{IJ} + I_3 \lambda_{(A)}^{-2} C_{IJ}^{-1}}{D_{(A)}} \tag{4}$$

Here, obviously, $D_{(A)}$ and $M_{IJ}^{(A)}$ must satisfy:

$$\sum_{A=1}^{3} \frac{1}{D_{(A)}} = 0 \quad ; \quad \sum_{A=1}^{3} \frac{\lambda_{(A)}^2}{D_{(A)}} = 0 \quad ; \quad \sum_{A=1}^{3} \frac{\lambda_{(A)}^4}{D_{(A)}} = 1$$

$$\sum_{A=1}^{3} M_{IJ}^{(A)} = C_{IJ}^{-1} \quad ; \quad \sum_{A=1}^{3} \lambda_{(A)}^2 M_{IJ}^{(A)} = \delta_{IJ} \quad ; \quad \sum_{A=1}^{3} \lambda_{(A)}^4 M_{IJ}^{(A)} = C_{IJ} \tag{5}$$

In the case that two or three principal stretches are equal, the value of $D_{(A)}$ (from Equation 3) becomes zero. This necessitates closer inspection of equations which rely on $D_{(A)}$ in the denominator.

Special Case $\lambda = \lambda_1 = \lambda_2 \neq \lambda_3$. In this case, which applies, for example to a uniaxial stretching of materials, one obtains for the deformation tensor

$$C_{IJ}^m = \lambda^{2m}(\delta_{IJ} - N_I^{(3)} N_J^{(3)}) + \lambda_3^{2m} N_I^{(3)} N_J^{(3)} \tag{6}$$

while the tensor $M_{IJ}^{(3)}$, used to calculate the product of deformation tensor's eigenvectors ($N_I^{(A)} N_J^{(A)} = \lambda_{(A)}^2 M_{IJ}^{(A)}$), is now

$$M_{IJ}^{(3)} = \frac{C_{IJ} - \left(I_1 - \lambda_3^2\right) \delta_{IJ} + I_3 \lambda_3^{-2} C_{IJ}^{-1}}{D_{(3)}} \tag{7}$$

Special Case $\lambda = \lambda_1 = \lambda_2 = \lambda_3$. For this special case, as found in hydrostatic stretching of materials, one obtains:

$$C^m_{IJ} = \lambda^{2m}\delta_{IJ} \tag{8}$$

2.2. Stress Measures

The second Piola–Kirchhoff stress is physically defined as the force per undeformed area loaded on a surface in the undeformed reference configuration:

$$S_{IJ} = 2\frac{\partial W}{\partial C_{IJ}} = \underbrace{w_A (M^{(A)}_{IJ})_A}_{\text{isochoric}} + \underbrace{\frac{\partial^{vol} W(J)}{\partial J} J\, C^{-1}_{IJ}}_{\text{volumetric}} \tag{9}$$

where w_A can be expressed as (for detailed derivation see Jeremić [5] and Holzapfel [3])

$$w_A = -\frac{1}{3}\,\frac{\partial^{iso} W}{\partial \tilde{\lambda}_B}\,\tilde{\lambda}_B\ + \frac{\partial^{iso} W}{\partial \tilde{\lambda}_{(A)}}\,\tilde{\lambda}_{(A)} \tag{10}$$

It should be noted that $\tilde{\lambda} = J^{-1/3}\lambda$ is the isochoric component of the principal stretch. The elastic potential function W is used to specify material models. The isochoric components of stress tensor will be affected by special cases of two or three equal stretches.

Special Case $\lambda = \lambda_1 = \lambda_2 \neq \lambda_3$. In this special case, the isochoric components of the second Piola Kirchhoff stress is

$$^{iso}S_{IJ} \quad = \quad w_3 M^{(3)}_{IJ} + w_1 (C^{-1}_{IJ} - M^{(3)}_{IJ}) \tag{11}$$

where $M^{(3)}_{IJ}$ is given by the Equation (7).

Special Case $\lambda = \lambda_1 = \lambda_2 = \lambda_3$. This is actually a trivial case as there is no isochoric stress from volumetric deformation

$$^{iso}S_{IJ} \quad = \quad 0 \tag{12}$$

It is worth noting that other stress measures are easily obtained once the Second Piola–Kirchhoff stress is known. For example, the First Piola–Kirchhoff stress is simply obtained from $P_{iJ} = F_{iK} S_{KJ}$, Cauchy stress is $\sigma_{ij} = 1/J \; F_{iM} S_{MN} F_{jN}$, Mandel stress is $T_{IJ} = C_{IK} S_{KJ}$, and the Kirchhoff stress is $\tau_{ij} = F_{iA} (F_{jB})^t S_{AB}$.

2.3. Constitutive Tangent Tensor

Material tangent stiffness relation is defined from:

$$dS_{IJ} = \frac{1}{2} \mathcal{L}_{IJKL} \, dC_{KL} \quad ; \quad \mathcal{L}_{IJKL} = 4 \, \frac{\partial^2 \left({}^{vol}W \right)}{\partial C_{IJ} \, \partial C_{KL}} + 4 \, \frac{\partial^2 \left({}^{iso}W \right)}{\partial C_{IJ} \, \partial C_{KL}} \tag{13}$$

with the definition of volumetric component of the stiffness tensor

$${}^{vol}\mathcal{L}_{IJKL} = (J^2 \frac{\partial^{2\,vol} W(J)}{\partial J \partial J} + \; J \frac{\partial^{vol} W(J)}{\partial J}) C^{-1}_{IJ} C^{-1}_{KL} + \; 2J \frac{\partial^{vol} W(J)}{\partial J} I^{C^{-1}}_{IJKL} \tag{14}$$

General case $\lambda_1 \neq \lambda_2 \neq \lambda_3$. In a general case, when the principal stretches are all different, one can write the isochoric part of the stiffness tensor as:

$$\mathcal{L}^{iso}_{IJKL} = Y_{AB} \; (M^{(B)}_{KL})_B \; (M^{(A)}_{IJ})_A + 2 \; w_A \; (\mathcal{M}^{(A)}_{IJKL})_A \tag{15}$$

where tensor Y_{AB} can be expressed as (for detailed derivation see Jeremić [4])

$$\begin{aligned} Y_{AB} = & \frac{\partial^{iso} W}{\partial \tilde{\lambda}_{(A)}} \, \delta_{(A)(B)} \; \tilde{\lambda}_{(B)} + \frac{\partial^{2\,iso} W}{\partial \tilde{\lambda}_{(A)} \partial \tilde{\lambda}_{(B)}} \; \tilde{\lambda}_{(A)} \; \tilde{\lambda}_{(B)} - \frac{1}{3} \left(\frac{\partial^{iso} W}{\partial \tilde{\lambda}_{(A)}} \; \tilde{\lambda}_{(A)} + \frac{\partial^{iso} W}{\partial \tilde{\lambda}_{(B)}} \; \tilde{\lambda}_{(B)} \right) \\ & - \frac{1}{3} \left(\frac{\partial^{2\,iso} W}{\partial \tilde{\lambda}_{(A)} \partial \tilde{\lambda}_D} \; \tilde{\lambda}_{(A)} \tilde{\lambda}_D + \frac{\partial^{2\,iso} W}{\partial \tilde{\lambda}_C \partial \tilde{\lambda}_{(B)}} \; \tilde{\lambda}_C \; \tilde{\lambda}_{(B)} \right) + \frac{1}{9} \left(\frac{\partial^{2\,iso} W}{\partial \tilde{\lambda}_C \partial \tilde{\lambda}_D} \; \tilde{\lambda}_C \; \tilde{\lambda}_D + \frac{\partial^{iso} W}{\partial \tilde{\lambda}_D} \; \tilde{\lambda}_D \right) \end{aligned} \tag{16}$$

The Simo–Serrin fourth order tensor $\mathcal{M}_{IJKL} = \partial M^{(A)}_{IJ} / \partial C_{KL}$ (eg. Morman [8] and Simo and Taylor [18]) is defined as:

$$\begin{aligned} \mathcal{M}^{(A)}_{IJKL} \;\; = \;\; & \frac{1}{D_{(A)}} \, (I_{IJKL} - \delta_{IJ} \delta_{KL} + \lambda^2_{(A)} (\delta_{IJ} M^{(A)}_{KL} + M^{(A)}_{IJ} \delta_{KL}) \\ + \;\; & I_3 \lambda^{-2}_{(A)} (C^{-1}_{IJ} C^{-1}_{KL} + I^{C^{-1}}_{IJKL} - C^{-1}_{IJ} M^{(A)}_{KL} - M^{(A)}_{IJ} C^{-1}_{KL}) - d_A M^{(A)}_{IJ} M^{(A)}_{KL}) \end{aligned} \tag{17}$$

The associated fourth order tensors $I^{C^{-1}}_{IJKL}$ and I_{IJKL} are defined as

$$I^{C^{-1}}_{IJKL} = -\frac{1}{2}\left(C^{-1}_{IK}C^{-1}_{JL} + C^{-1}_{IL}C^{-1}_{JK}\right) \quad ; \quad I_{IJKL} = \frac{1}{2}\left(\delta_{IK}\delta_{JL} + \delta_{IL}\delta_{JK}\right) \tag{18}$$

By using equations (5), one observes that $\mathcal{M}^{(A)}_{IJKL}$ satisfies

$$\sum_{A=1}^{3} \mathcal{M}^{(A)}_{IJKL} = I^{C^{-1}}_{IJKL} \quad ; \quad \sum_{A=1}^{3} \lambda^2_{(A)}\mathcal{M}^{(A)}_{IJKL} + \sum_{A=1}^{3} \lambda^2_{(A)} M^{(A)}_{IJ} M^{(A)}_{KL} = 0$$
$$\sum_{A=1}^{3} \lambda^4_{(A)}\mathcal{M}^{(A)}_{IJKL} + 2\sum_{A=1}^{3} \lambda^4_{(A)} M^{(A)}_{IJ} M^{(A)}_{KL} = I_{IJKL} \tag{19}$$

Special case $\lambda = \lambda_1 = \lambda_2 \neq \lambda_3$. In this special case the stiffness tensor is obtained as:

$$\begin{aligned} \mathcal{L}^{iso}_{IJKL} &= Y_{33} M^{(3)}_{IJ} M^{(3)}_{KL} + Y_{11}\left(C^{-1}_{IJ} - M^{(1)}_{IJ}\right)\left(C^{-1}_{KL} - M^{(1)}_{KL}\right) \\ &+ Y_{13}\left(C^{-1}_{IJ} - M^{(1)}_{IJ}\right) M^{(3)}_{KL} + Y_{31} M^{(3)}_{IJ}\left(C^{-1}_{KL} - M^{(1)}_{KL}\right) \\ &+ 2w_3\mathcal{M}^{(3)}_{IJKL} + 2w_1(I^{C^{-1}}_{IJKL} - \mathcal{M}^{(3)}_{IJKL}) \end{aligned} \tag{20}$$

Special case $\lambda = \lambda_1 = \lambda_2 = \lambda_3$. For this special case the stiffness tensor collapses to the following form:

$$\mathcal{L}^{iso}_{IJKL} = 2G\lambda^{-4}\left(I_{IJKL} - \frac{1}{3}\delta_{IJ}\delta_{KL}\right) \tag{21}$$

Remark. For the small deformation case (where $\lim_{\lambda\to1} C_{ij} = \delta_{ij}$; $\lim_{\lambda\to1} J = 1$) the stiffness tensor collapses to

$$\mathcal{L}_{IJKL} \to E_{ijkl} = (K_b - 2/3\ G)\,\delta_{ij}\delta_{kl} + (2G)I_{ijkl} \tag{22}$$

This is exactly the small deformation linear elastic stiffness tensor in terms of bulk modulus K_b and shear modulus G.

2.4. Perturbation Technique.

One of the suggested techniques for resolving cases of two or three equal principal stretches is based on perturbations (eg. Simo [15]). This technique should be carefully utilized as in some cases inconsistent results are obtained. This is illustrated on a set of analytical experiments.

Let us assume an initial state of deformation given by

$$F_{iJ} = C_{IJ} = \delta_{ij} \quad \Rightarrow \quad \lambda_1 = \lambda_2 = \lambda_3 = 1$$

Since this state represents total lack of deformation, the large deformation constitutive stiffness tensor should be the same as that one for small deformations.

A perturbation $\chi = \alpha\sqrt{M}$ is introduced to the principal stretches λ_1, λ_2 and λ_3 to distinctly separate their values. Here M is the machine precision[‡] and α is a factor. On our computer platform (Intel Pentium CPU), the square root of machine precision is $\sqrt{M} = 3.293 \times 10^{-10}$.

A perturbation of equal principal stretches of the form

$$\lambda_1 = 1 + \chi \quad ; \quad \lambda_2 = 1 \quad ; \quad \lambda_3 = 1 - \chi$$

is assumed and used for calculation of the constitutive tensor. This state of principal stretches is essentially a small deformation configuration and both large and small deformation theories

[‡] Machine precision or machine epsilon (*macheps*) is the smallest distinguishable positive number (in a given precision, i.e. float (32 bits), double (64 bits) or long double (80 bits), such that $1.0 + macheps > 1.0$ yields true on the given computer platform. The ANSI/IEEE Standard 754-1985, defines *macheps* for a number of floating point precisions. For example, double precision $macheps = 2.22 \times 10^{-16}$, while the long double $macheps = 1.08 \times 10^{-19}$. Curiously enough, Intel 80x86 platform promotes all the float, double and long double precision numbers to long number inside the floating point unit (FPU) and all the computations are performed using 80 bits of precision. Results are then truncated to predefined predefined precision upon exiting the FPU. Consequence is that one is forced to use the highest precision macheps on Intel 80x86 even if it might not be portable.

should give the same result. Given bulk modulus $K_b = 1.9717$ MPa and shear modulus $G = 0.4225$ MPa, and using the definition for small deformation linear elastic stiffness tensor in equation (22), a few illustrative stiffness values are given in Table (I).

Table I. Selected small deformation (SD) and large deformation (LD) stiffness components for different perturbation numbers. Units are Pascals [Pa].

SD Stiffness component (Eq. (22))	E_{1111}	E_{1122}	E_{1212}
(reference values)	2.530×10^6	1.690×10^6	4.225×10^5
Perturbation / LD Stiffness component	$\mathcal{L}_{1111}$	$\mathcal{L}_{1122}$	$\mathcal{L}_{1212}$
$\alpha = 10^0, 10^1$	NaN	NaN	NaN
$\alpha = 10^2$	2.710×10^6	2.031×10^6	3.396×10^5
$\alpha = 10^3, 10^4, 10^5$	2.711×10^6	2.035×10^6	3.396×10^5

The reason for the differences and in some cases lack of results[§] can be attributed to the fact that C_{IJ}, C_{IJ}^{-1} and $I_{IJKL}^{C^{-1}}$ remain unperturbed, while λ_1, λ_2, and λ_3 are perturbed. This inconsistency produces a difference, and may result in erroneous results. A simple check why the perturbation method does not work is obtained by verifying that identities given by equations (5) and (19) are not satisfied after perturbation.

3. NUMERICAL EXAMPLES

A set of two representative examples is provided to illustrate closed form solutions derived above. The examples are related to uniaxial tension and volumetric deformation, since those

[§]The NaN means Not a Number and is essentially a result of a numerical value overflowing the largest accurate representation of any number in given accuracy cases are usually found in formulation verifications and model validations. It is noted that the examples described and analyzed below will fail to yield results (numerical overflow) or will yield wrong results (see Table I) if the perturbation technique is used. The assumed material properties (for small deformation model) are Young's modulus $E = 1.183 \times 10^6$ Pa and Poisson's Ratio $\nu = 0.4$ (which gives bulk modulus $K_b = 1.9717$ MPa and shear modulus $G = 0.4225$ MPa). Related material constants for the Ogden material model (using the parameters from Ogden [10]) are: $N = 3$, $\mu_1 = 1.3$, $\mu_2 = 5.0$, $\mu_3 = -2.0$, $c_1 = 6.3 \times 10^5$ Pa, $c_2 = 1.2 \times 10^3$ Pa, $c_1 = -1.0 \times 10^4$ Pa . The parameters for the Mooney–Rivlin material model (as suggested by Anand [1]) are: $C_1 = (7/16)G$, $C_2 = (1/16)G$.

Uniaxial tension. The case of uniaxial tension (or compression, as in soil mechanics tests) has two equal principal stretches, $\lambda_1 > \lambda_2 = \lambda_3 = \lambda$. Since the material is compressible ($\mu = 0.4$) and the constraint is uniaxial, $\lambda_1 > 1$, $\lambda < 1$, the only nonzero stress component is σ_{11}.

Figure (1) shows that the tensile tractions (undeformed reference) increases with the increase of tensile stretch for the Neo–Hookean, Logarithmic, Mooney–Rivlin–Simo and Ogden–Simo model. It is interesting to note that the logarithmic model response exhibits softening in response (tractions vs. stretch) caused by the violation of Legendre–Hadamard condition (eg. Bruhns et al. [2]).

Volumetric deformation. Volumetric deformation has three equal principal stretches, $\lambda_1 = \lambda_2 = \lambda_3 = \lambda$. Only volumetric stress $p_m = \sigma_{11} = \sigma_{22} = \sigma_{33}$ is nonzero. The volume ratio $J = \lambda_1\lambda_2\lambda_3$ is used to represent volumetric deformation. The absence of volumetric deformation is implied by $J = 1$. Volumetric dilation applies when $J > 1$, while the volumetric

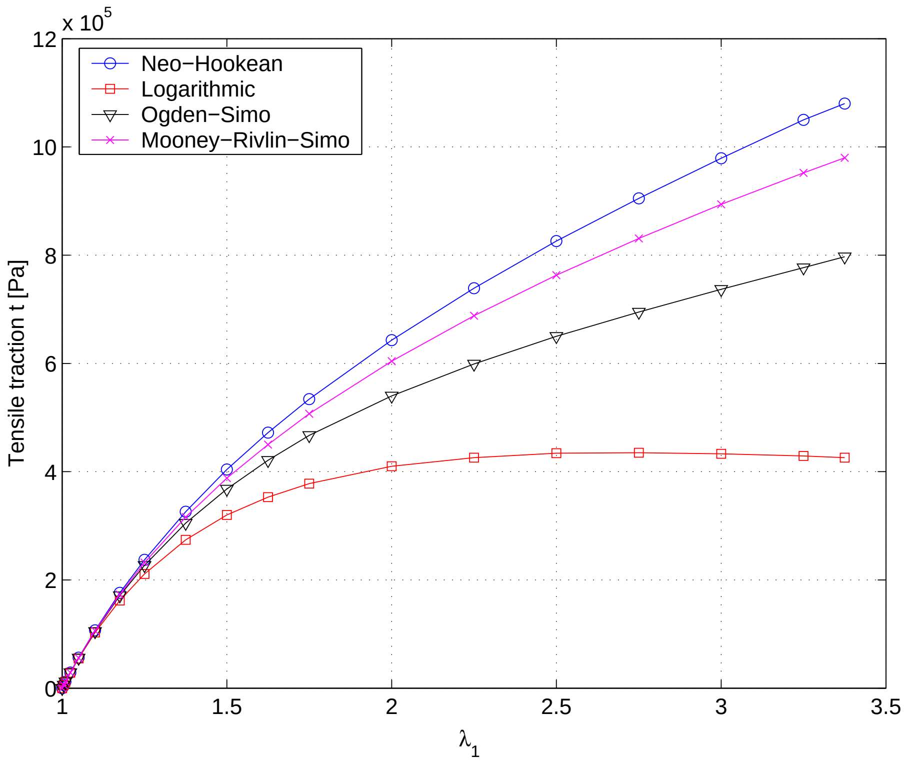

Figure 1. Uniaxial tension: tensile traction t (undeformed reference) vs. tensile stretch λ_1

contraction holds when $0 < J < 1$.

Figure (2) shows the volumetric traction (undeformed reference) versus volume ratio, respectively for the Neo–Hookean, Logarithmic, and Simo–Pister models. These curves have the same slope when $J = 1$, which is expected as the deformations approach the small deformation case.

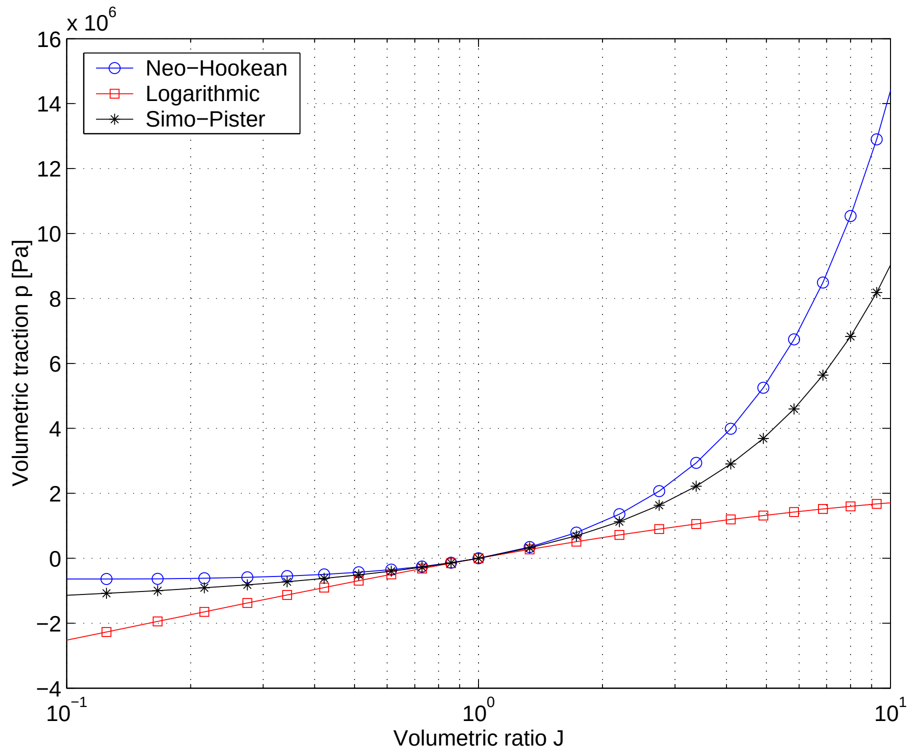

Figure 2. Volumetric deformation: hydrostatic pressure p (undeformed reference) vs. volume ratio J

4. CONCLUSIONS

A common deformation state with two or three equal principal stretches in computational hyperelasticity was investigated. A closed form solutions for deformation measures, stress measures and stiffness tensor were analytically presented in Lagrangian format. These solutions are particularly important in view of possible problems with perturbation techniques that are used to overcome computational difficulties. An example of illustrating problems with perturbation technique shows that even when a solution is available, it might be the wrong one. In addition to that, a set of numerical examples, employing presented analytical solutions was used as an illustration for cases with two or three equal principal stretches.

Of particular importance is a decisions on when to consider principal stretches equal. This decisions has to be made within computational implementation of large deformation hyperelasticity. A simple suggestion is that if the difference between two or three principal stretches is within a value of $\chi^{\star} = 10^2\sqrt{M}$, they can be treated as numerically equal and the analytical formulae for two or three equal principal stretches (developed in this paper) should be used.

We also note that the described theory is implemented into the public domain finite element platform OpenSees (eg. [11]) with the source code and above examples available on-line.

Acknowledgment

This work was supported in part by a number of grants listed below: Earthquake Engineering Research Centers Program of the National Science Foundation under Award Number EEC-9701568 (cognizant program director Dr. Joy Pauschke); Civil and Mechanical System program, Directorate of Engineering of the National Science Foundation, under Award NSF-CMS-0337811 (cognizant program director Dr. Steve McCabe);

REFERENCES

1. Anand, L. Moderate deformations in extension-torsion of incompressible isotropic elastic materials. *Journal of the mechanics and Physics of Solids 34* (1986), 293–304.
2. Bruhns, O., Xiao, H., and Meyers, A. Constitutive inequalities for an isortopic elastic strain–energy function based on Hencky's logarithmic strain tensor. *Procedings of the Royal Society A, London 457* (2001), 2207–2226.
3. Holzapfel, G. A. *Nonlinear Solid Mechanics: a continuum approach for engineering.* John Wiley & Sons, Ltd., New York, 2001.
4. Jeremić, B. *Finite Deformation Hyperelasto–Plasticity of Geomaterials.* PhD thesis, University of Colorado at Boulder, July 1997.
5. Jeremić, B., Runesson, K., and Sture, S. Finite deformation analysis of geomaterials. *International Journal for Numerical and Analytical Methods in Geomechanics including International Journal for Mechanics of Cohesive–Frictional Materials 25*, 8 (2001), 809–840.
6. Lee, E. H., and Liu, D. T. Finite–strain elastic–plastic theory with application to plane–wave analysis. *Journal of Applied Physics 38*, 1 (January 1967), 19–27.
7. Miehe, C. Aspects of the formulation and finite element implementation of large strain isotropic elasticity. *International Journal for Numerical Methods in Engineering 37* (1994), 1981–2004.
8. Morman, K. N. The generalized strain meassures with application to nonhomogeneous deformation in rubber–like solids. *Journal of Applied Mechanics 53* (1986), 726–728.
9. Oberkampf, W. L., Trucano, T. G., and Hirsch, C. Verification, validation and predictive capability in computational engineering and physics. In *Proceedings of the Foundations for Verification and Validation on the 21st Century Workshop* (Laurel, Maryland, October 22-23 2002), Johns Hopkins University / Applied Physics Laboratory, pp. 1–74.
10. Ogden, R. W. *Non–Linear Elastic Deformations.* Series in mathematics and its applications. Ellis Horwood Limited, Market Cross House, Cooper Street, Chichester, West Sussex, PO19 1EB, England, 1984.
11. OpenSees Development Team (Open Source Project). OpenSees: open system for earthquake engineering simulations. `http://opensees.berkeley.edu/`, 1998-2004.
12. Roache, P. J. *Verification and Validation in Computational Science and Engineering.* hermosa publishers, 1998. ISBN 0-913478-08-3.
13. Simo, J. C. A framework for finite strain elastoplasticity based on maximum plastic dissipation and the multiplicative decomposition: Part i. continuum formulation. *Computer Methods in Applied Mechanics and Engineering 66* (1988), 199–219. TA345. C6425.
14. Simo, J. C. A framework for finite strain elastoplasticity based on maximum plastic dissipation and the multiplicative decomposition: Part ii. computational aspects. *Computer Methods in Applied Mechanics and Engineering 68* (1988), 1–31. TA345. C6425.
15. Simo, J. C. Algorithms for static and dynamic multiplicative plasticity that preserve the classical return mapping schemes of the infinitesimal theory. *Computer Methods in Applied Mechanics and Engineering 99* (1992), 61–112.
16. Simo, J. C., and Ortiz, M. A unified approach to finite deformation elastoplastic analysis based on the use of hyperelastic constitutive equations. *Computer Methods in Applied Mechanics and Engineering 49* (1985), 221–245.
17. Simo, J. C., and Pister, K. S. Remarks on rate constitutive equations for finite deformations problems: Computational implications. *Computer Methods in Appliied Mechanics and Engineering 46* (1984), 201–215.
18. Simo, J. C., and Taylor, R. L. Quasi–incompressible finite elasticity in principal stretches. continuum basis and numerical algorithms. *Computer Methods in Applied Mechanics and Engineering 85* (1991), 273–310.
19. Ting, T. C. T. Determination of $C^{1/2}$, $C^{-1/2}$ and more general isotropic tensor functions of C. *Journal of Elasticity 15* (1985), 319–323.

APPENDIX

II. Isotropic Hyperelastic Models

Derivatives needed to obtain stiffness tensors and stress measures for a set of hyperelastic models are given in Table (II). Detail descriptions for these models can be found in Ogden [10], Miehe [7] and Simo and Marsden [17].

Table II. Derivatives for stiffness tensors and stress measures of various hyperelastic material models.

Model	$\frac{\partial^{iso}W}{\partial\tilde{\lambda}_A}$	$\frac{\partial^2\left({}^{iso}W\right)}{\partial\tilde{\lambda}_A^2}$	$\frac{d^{vol}W(J)}{dJ}$	$\frac{d^{2\,vol}W(J)}{dJ^2}$
Ogden	$\sum_{r=1}^{N} c_r\tilde{\lambda}_A^{\mu_r-1}$	$\sum_{r=1}^{N} c_r(\mu_r-1)\tilde{\lambda}_A^{\mu_r-2}$		
Neo-Hookean	$G\tilde{\lambda}_A$	G	$K_b(J-1)$	K_b
Mooney–Rivlin	$2C_1\tilde{\lambda}_A - 2C_2\tilde{\lambda}_A^{-3}$	$2C_1 + 6C_2\tilde{\lambda}_A^{-4}$		
Logarithmic	$2G\tilde{\lambda}_A^{-1}\ln\tilde{\lambda}_A$	$2G\tilde{\lambda}_A^{-2}(1-\ln\tilde{\lambda}_A)$	$K_bJ^{-1}\ln J$	$K_bJ^{-2}(1-\ln J)$
Simo–Pister			$(J-\frac{1}{J})\frac{K_b}{2}$	$(1+\frac{1}{J^2})\frac{K_b}{2}$